Available online at www.sciencedirect.com
SCIENCE DIRECT®
Journal of the European Ceramic Society 25 (2005) 1215–1223
www.elsevier.com/locate/jeurceramsoc

Mechanical properties of melt-grown Al_2O_3–$ZrO_2(Y_2O_3)$ eutectics with different microstructure

J.Y. Pastor[a], J. LLorca[a,*], P. Poza[a,1], I. de Francisco[b], R.I. Merino[b], J.I. Peña[b]

[a] *Department of Materials Science, Polytechnic University of Madrid, E.T.S. de Ingenieros de Caminos, 28040 Madrid, Spain*
[b] *Instituto de Ciencia de Materiales de Aragón, C.S.I.C., Universidad de Zaragoza, 50009 Zaragoza, Spain*

Available online 2 February 2005

Abstract

The effect of the microstructure on the mechanical properties of Al_2O_3–$ZrO_2(Y_2O_3)$ eutectic ceramic oxides was studied. Rods processed by the laser-heated floating zone method with three different microstructures were obtained as the growth rate increased: a homogeneous dispersion of irregular ZrO_2 lamellae within the Al_2O_3 matrix, colonies with a core containing a dispersion of submicron ZrO_2 lamellae or rods surrounded by a thick intercolony region, and elongated cells formed by a dispersion of very fine ZrO_2 lamellae and separated by thin intercellular boundaries. The average flexure strength (close to 1.6 GPa) of the eutectics made up of a homogeneous dispersion of ZrO_2 lamellae was outstanding, and they also presented an excellent Weibull modulus (12.9) when the microstructure was homogeneous throughout the sample. Banding did not affect the average strength but degraded the Weibull modulus. In general, the flexure strength decreased as the size of the main morphological features of the microstructure (colony or cell diameter) increased. The thickness of the intercellular boundaries increased with the Y_2O_3 content and, above a critical value, reduced dramatically the strength by activating a new failure mechanism based on the coalescence of the pores and shrinkage cavities concentrated at the intercellular boundaries.

Keywords: Eutectic oxides; Mechanical properties; Strength; Microstructure; Hardness

1. Introduction

Directionally solidified eutectic ceramic oxides based on the Al_2O_3–$ZrO_2(Y_2O_3)$ system processed in the mid 1970s presented very little degradation in strength up to 1500 °C.[1] This was attributed to the eutectic character of the microstructure, which was formed by a dispersion of ZrO_2 rods or platelets in a continuous Al_2O_3 matrix, which generally grew with the *c*-axis parallel to the solidification direction. The outstanding creep resistance of sapphire along the *c*-axis and the clean, strong grain boundaries produced during the eutectic solidification contributed to the retention of the mechanical strength even at very high temperature. Additionally, the interfaces in the eutectic are mostly low energy ones and hence thermodynamically stable at high temperature. These results were confirmed by later studies[2–4] but these were of less importance because the ambient temperature strength of the eutectic ceramic oxide was modest (below 500 MPa). However, significant improvements in the processing techniques during the last 10 years have produced a new generation of directionally solidified Al_2O_3–$ZrO_2(Y_2O_3)$ eutectics whose ambient temperature strength surpasses 1 GPa.[4–8] The high temperature strength of these enhanced materials was studied by Sayir et al.[9] and more recently by Pastor et al.,[8,10] who reported excellent strength retention and creep resistance up to 1400 °C.

These results indicate that improvements in the ambient temperature strength can be readily translated to high temperature, and further improvements in the mechanical behavior can be expected by controlling the processing conditions and the eutectic composition to obtain an optimum microstructure. This requires systematic investigations to establish the relationship between the microstructure and the deformation

* Corresponding author. Tel.: +34 913 365 375; fax: +34 915 437 845.
E-mail address: jllorca@mater.upm.es (J. LLorca).
[1] Present address: Escuela Politécnica Superior, Universidad Rey Juan Carlos, 28993 Móstoles, Spain.

0955-2219/$ – see front matter © 2005 Elsevier Ltd. All rights reserved.
doi:10.1016/j.jeurceramsoc.2005.01.004

and failure micromechanisms, but very few studies of this type have been carried out. The effect of Y_2O_3 content on the strength was recently addressed for eutectic[10] and hypoeutectic compositions,[11] and both studies found the best performance when the fraction of Y_2O_3 dissolved into the ZrO_2 was around 3 mol%. The tetragonal ZrO_2 grains did not transform into the monoclinic polymorph during deformation and the strength was provided by the continuous Al_2O_3 phase, which was subjected to high compressive residual stresses as a result of the mismatch in the thermal expansion coefficients of α-Al_2O_3 and tetragonal ZrO_2. Eutectics with higher Y_2O_3 content presented similar mechanical properties and the strength decreased only very slightly. On the contrary, the spontaneous martensitic transformation of the ZrO_2 grains upon cooling in the samples with low Y_2O_3 content led to the formation of interface microcracks, which grew into the Al_2O_3 phase driven by the tensile residual stresses generated by the volumetric strain associated with the transformation. The large defects formed by the coalescence of microcracks reduced the strength by almost 50% at ambient temperature, and the degradation of the mechanical properties was more noticeable at high temperature.

In this investigation, Al_2O_3–$ZrO_2(Y_2O_3)$ eutectic rods were processed by the laser-heated floating zone method at different growth rates to change systematically the microstructure from a homogeneous dispersion of irregular ZrO_2 lamellae to a colony structure and then to a cellular structure. Moreover, banding inhomogeneities—often found in eutectics grown by this method—were present in some rods. We studied the effect of morphology and of the inhomogeneities in the microstructure on the ambient temperature flexure strength and Weibull modulus, and ascertained the defects limiting the strength. This led to the identification of the critical microstructural parameters, which determine the strength of this family of eutectic ceramic oxides.

2. Processing and experimental techniques

The materials were prepared from commercial powders of ZrO_2 (Alfa 99%), Y_2O_3 (Aldrich 99.99%) and Al_2O_3 (Aldrich 99.99%), and contained 63 mol% of Al_2O_3 and 37 mol% of a mixture of ZrO_2 and Y_2O_3. Powders with different nominal Y_2O_3 content were prepared and the proportion of Y_2O_3 was always expressed by Y = mol% Y_2O_3/(mol% ZrO_2 + mol% Y_2O_3). They were milled in a vibratory micromill (model MM2000, Resch, Haan, Germany) with acetone, using alumina components, fired in air at 1000 °C for 1 h, hand milled in an agate mortar and mixed in the desired composition. The precursor rods were made by isostatic pressing of the powder mixtures at 200 MPa and at ambient temperature, followed by sintering at 1500 °C to increase the density to 65% of the theoretical one and to provide handling strength.

Directionally solidified eutectic rods were obtained by the laser-heated floating zone method using a CO_2 laser. Pulling the rods downwards from a low-density ceramic precursor creates bubbles in the melt that lead to holes and voids in the as-grown rod. The rods were first grown upwards at 200 mm/h at a rotation speed of 50 rpm to get high density and homogeneous precursors. The final eutectic rods were then grown downwards at different growth rates, as indicated in Table 1. More details of the processing can be found elsewhere.[12,13] Rods of 50–100 mm in length and 1.2–1.6 mm in diameter were obtained.

Table 1
Processing parameters for each batch of eutectic rods

	Denomination				
	L3	L12	Co9	C3	C12
Growth rate (mm/h)	20	20	30	1000	1000
Y (%) = mol% Y_2O_3/(mol% ZrO_2 + mol% Y_2O_3)	3	12	9	3	12

Longitudinal and transversal sections were cut from the rods using a diamond saw, and polished first with diamond of 30 μm grain size as abrasive, and then with a diamond slurry (up to 1 μm). The polished surfaces were cleaned in deionized water, and subsequently by ultrasound in butanone and ethanol. The surfaces were coated with a thin layer of Au–Pd and the microstructure was observed in a JEOL 6300 scanning electron microscope (SEM) equipped with energy-dispersive X-ray microanalysis. Secondary and back-scattered electron detectors were used to ascertain the characteristics of the microstructure along the rod and across the diameter. Quantitative information on the morphology of the ZrO_2 lamellae, colony and cell dimensions, etc. were obtained from the digitized back-scattered electron images using an image analysis program and the mean-intercept method.

The flexure strength of the rods in the longitudinal direction was measured in three-point bending tests with 8.5 mm loading span carried out in an Instron 4505 servo-mechanical testing machine. All the tests were performed in air under stroke control at a cross-head speed of 50 μm per minute. The flexure strength was computed from the maximum load in the test according to the Strength of Materials theory for an elastic beam of circular section. In addition, the Vickers hardness was measured on the longitudinal and transverse polished sections with a microhardness tester (Akashi MVK-E II) under a load of 9.8 N.

3. Microstructure

Longitudinal and transversal sections were examined in the SEM to determine the microstructural characteristics of the rods. X-ray microanalysis in the SEM showed that the Y_2O_3 was dissolved into the ZrO_2 in all the materials and no amorphous phase or primary phase grains were detected. ZrO_2 phase was in tetragonal form in the eutectics with Y = 3% and 9% while the cubic polymorph was dominant in those with Y = 12%.[16] The samples grown at 20 mm/h

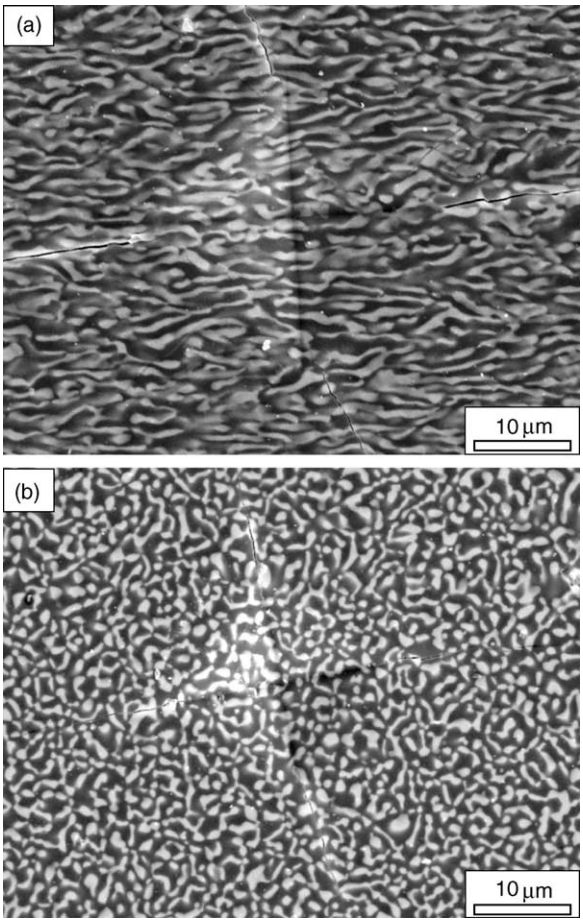

Fig. 1. Secondary electron micrographs of the L12 eutectic showing the homogeneous dispersion of irregular ZrO_2 lamellae (white) in the continuous Al_2O_3 matrix (dark grey). (a) Longitudinal section, the growth axis is horizontal. (b) Transverse section, the cracks induced by Vickers indentation are seen in both micrographs.

(denominated L3 and L12) were formed by a fine and homogeneous dispersion of irregular, elongated ZrO_2 lamellae oriented along the growth axis and embedded within a continuous Al_2O_3 matrix, as shown in Fig. 1. The average length and width of the lamellae (measured on longitudinal sections) together with the corresponding standard deviations are shown in Table 2, which also includes the average interlamella distance measured perpendicularly to the loading axis. This type of microstructure was already reported by other authors in Al_2O_3–$ZrO_2(Y_2O_3)$ eutectic rods grown at very low rates,[13–16] and it is characteristic of a planar solidification front where coupled growth takes place.

Neither the lamella morphology nor the spacing were significantly modified by the Y_2O_3 content, but the overall microstructure of the L3 and L12 eutectics showed some differences at other levels. The L3 rods presented bands perpendicular to the growth axis with a coarser microstructure (Fig. 2a). The Al_2O_3 content was higher within these bands, the ZrO_2 grains were bigger and often rounded in shape, as opposed to the fine, elongated lamellae found in the rest of the rod. The bands appeared every 60–70 μm and their average thickness was in the range 5–15 μm. These instabilities have been reported in rods grown at low speeds.[7,13,16] and arise from periodic perturbations in the melt (created by laser power fluctuations, axis hitches, etc.) which induce segregation or phase coarsening leading to band formation. The transition between the regions with fine, elongated lamellae and those with coarse, rounded ZrO_2 grains was very sharp, and this facilitated the nucleation of defects and cracks in these areas, as is shown in Fig. 2b. On the contrary, the microstructure of the L12 eutectic was extremely fine and homogeneous throughout the specimen, as is shown in Fig. 2c.

Dendrites start to develop in the rods grown at higher rate (30 mm/h), and a planar growth front was not maintained. This gave rise to colonies with ellipsoidal shape and the longer axis perpendicular to the solidification front in the material denominated Co9 (Fig. 3a). The colony aspect ratio (defined as the ratio between the major and minor axes of the ellipse) and the inclination from the rod axis increased with the distance to the center, due to the morphology of the solidification front, which forms a meniscus concave towards the solid phase. The center of each colony was formed by a disordered dispersion of fine ZrO_2 lamellae (Fig. 3b) or of ordered ZrO_2 rods of ≈0.3 μm in diameter (Fig. 3c). Although the orientation of each phase was not determined, this latter morphology is compatible with previous observations,[2,3,7,14] which indicated that the Al_2O_3 phase (which has the largest entropy of fusion) plays the leading role during solidification, growing along the *c*-axis with facets in the rhombohedral (1–102) planes while the ZrO_2 rods grew perpendicular to these planes and parallel to the Al_2O_3 *R* direction. This led to the ordered structure shown in Fig. 3c, where the ZrO_2 rods were distributed in three sets following the trigonal symmetry depicted in the transverse cross-section. The colony core was surrounded by a thick intercolony region formed by coarse ZrO_2 particles of irregular shape. Cracks and pores were often found in the intercolony region. The main morphological parameters of the colonies (average length and width) as well as the width of the intercolony

Table 2
Morphological parameters of the microstructure

	Denomination				
	L3	L12	Co9	*C*3	*C*12
Lamella/colony/cell length (μm)	2.3 ± 1.9	2.9 ± 2.1	≈90		
Lamella/colony/cell width (μm)	0.7 ± 0.4	0.8 ± 0.5	31 ± 10	18 ± 5	19 ± 5
Interlamella distance (μm)/intercolony/intercell thickness	1.8	1.6	13 ± 4	1.9 ± 0.6	2.7 ± 0.6

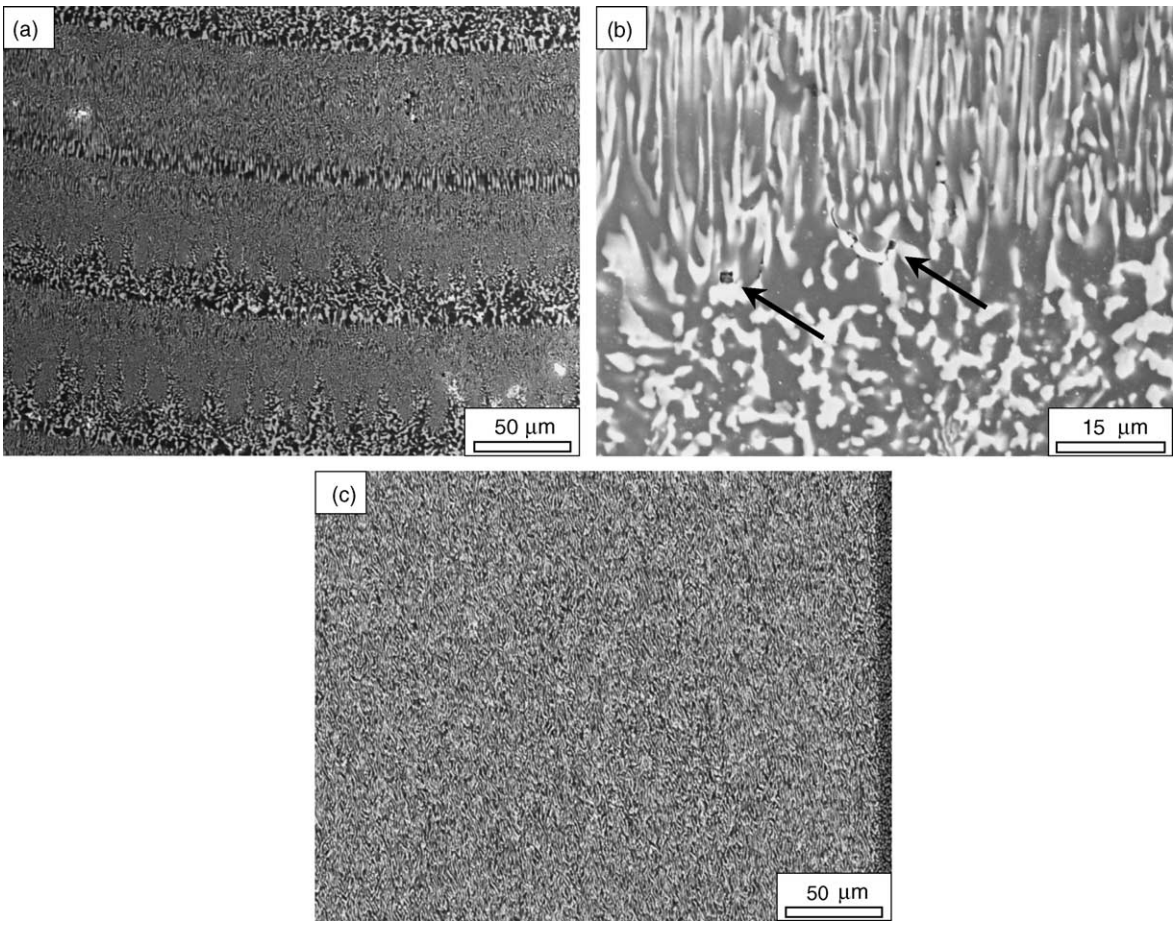

Fig. 2. (a) Longitudinal section of a L3 eutectic rod showing periodic banding perpendicularly to the growth axis. (b) Detail of the sharp transition between the bands with different microstructure. Cracks and pores are pointed by arrows. (c) Longitudinal section of a L12 eutectic rod showing the homogeneous microstructure without banding. The growth axis was vertical in all cases.

zones were measured and are given in the third column of Table 2.

The rods C3 and C12, grown at very high growth rates (1000 mm/h), showed a cellular structure made up by very elongated cells parallel to the growth axis (Fig. 4a). The microstructure within the cells was formed by very fine ZrO_2 lamellae resulting from the cooperative growth of both phases, as in the rods grown at 20 mm/h. However, the ZrO_2 lamellae in the rods grown at low rates were bigger and oriented along the growth axis (Fig. 1a). The lamellae obtained at 1000 mm/h were finer, and two different growth habits were found in each cell, the lamellae being tilted towards the intercellular boundaries (Fig. 4b). The morphology of the cells was measured on transverse cross-sections (Fig. 4c and d), and the average diameter as well as the intercellular boundary thickness is given in columns 4 and 5 of Table 2. The intercellular boundary was significantly thicker in the C12 eutectic, as already noted by other authors,[15] and this phenomenon was attributed to the Y_2O_3 segregation during solidification. Cracks and cavities were sometimes detected at the intercellular boundaries.

4. Mechanical properties

4.1. Average flexure strength

The average flexure strength (and the corresponding standard errors) of the eutectic rods is presented in Fig. 5. They were obtained from seven tests in all the materials except in C3 (23 tests) and Co9 (three tests) and plotted as a function of a characteristic length of each microstructure, which was taken as the average dimension of the feature, which defined the morphology of the microstructure perpendicularly to the tensile stress. Previous studies[5,10] showed that the strength was a function of the colony size, and the colony or cell diameter perpendicular to the growth axis was chosen as the characteristic length in rods with cellular (C3 and C12) and colony (Co9) microstructure. The selection of the characteristic length for the rods formed by a homogeneous distribution of ZrO_2 lamellae was not so obvious, and various candidates (lamellae width or interlamella distance) could be chosen. Both are of the order of one micron, and selecting one instead of the other does not change the plot significantly.

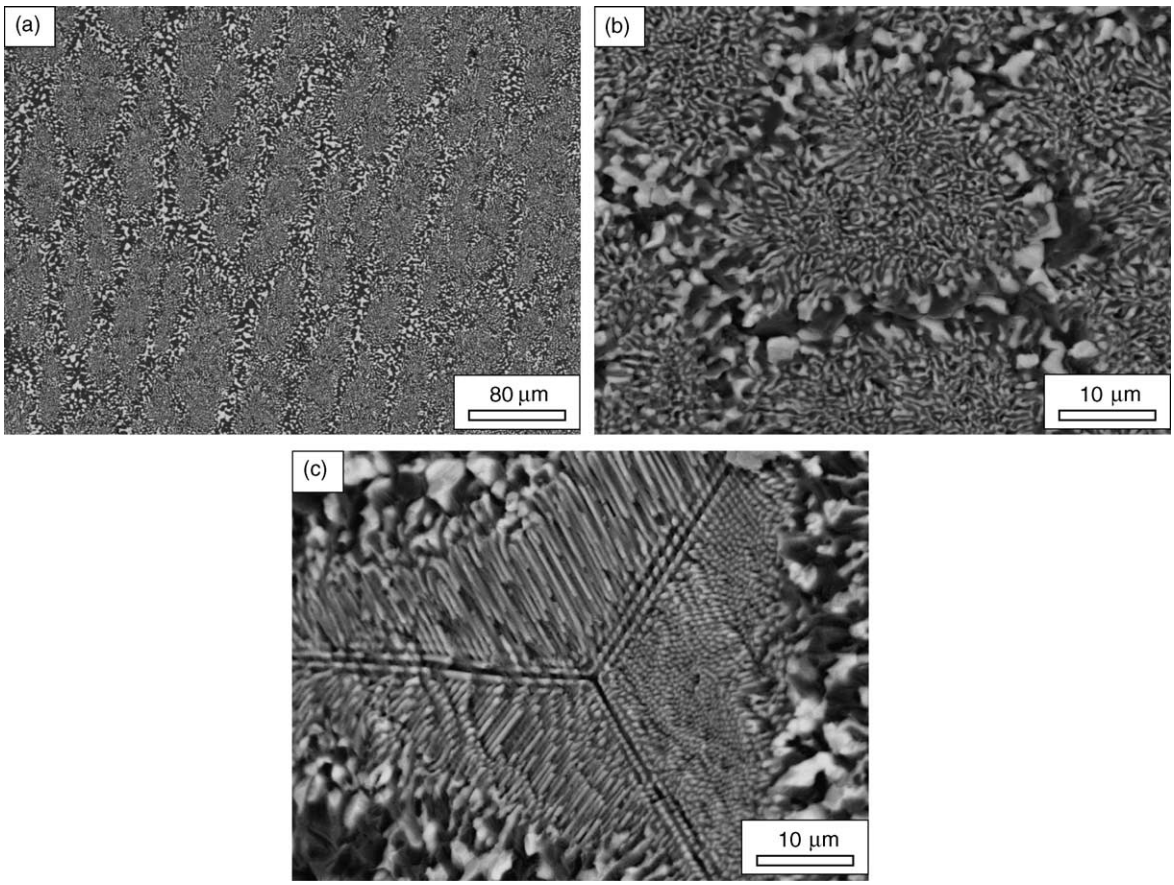

Fig. 3. Microstructure of the Co9 eutectic rods grown at 30 mm/h. (a) Longitudinal section showing the colonies oriented perpendicularly to the solidification front. (b) Transverse section showing a colony formed by a disordered dispersion of ZrO_2 lamellae surrounded by a coarse region with bigger ZrO_2 grains. (c) *Idem* for a colony formed by an ordered distribution of ZrO_2 rods. The micrographs were taken using back-scattered electrons to enhance the contrast between the phases.

The data in Fig. 5 show an increase in flexure strength as the colony or cell diameter decreased. This conclusion is supported by the flexure strengths measured by Bates[5] on Al_2O_3–$ZrO_2(Y_2O_3)$ eutectic fibers with Y = 9.5% prepared by the edge defined-film fed-growth method, which follow the trend indicated by our results. The only exception was the strength of the C12 rods, but the degradation in the mechanical properties can be explained by the analysis of fracture nucleating defects. Two representative fracture surfaces corresponding to the C3 and C12 eutectic rods are shown in Figs. 6 and 7, respectively. The C3 sample was broken at 1.48 GPa and the fracture surface presented the typical river patterns (Fig. 6a) pointing towards a surface defect of a few microns in size (Fig. 6b) which nucleated the crack. River patterns were not found on the fracture surface of the C12 specimen, which broke at 0.52 GPa. The fracture nucleating defect was, however, identified from the position of the rod surface under tensile stresses during bending; it is enclosed in a circle in Fig. 7a. An examination of this region at higher magnification showed that it was formed by a cell whose boundaries had been broken by the coalescence of small pores and microcracks, leading to a much larger defect and thus reducing the flexure strength.

These results show that the strength of Al_2O_3–$ZrO_2(Y_2O_3)$ eutectics with a cell (or colony) microstructure is very sensitive to the characteristics of the disordered intercellular regions. They are the last to solidify, and normally contain large ZrO_2 particles of irregular shape, pores and shrinkage cavities.[8,11] Shrinkage cavities appear when there is not enough liquid to flow into the intercellular regions, which are the last to solidify, because they are too far away from the solidification front. The volumetric shrinkage on cooling leads to the development of the shrinkage cavities with a crack-like morphology. This process is enhanced by the presence of Y_2O_3, and hence the thickness of the intercellular region (see Table 2) as well as the number of defects in this zone increase with Y_2O_3, as reported in several investigations.[8,11,15] Beyond a critical thickness, fracture is no longer nucleated at surface defects but is triggered by the coalescence of the pores and shrinkage cavities concentrated in the intercellular region, decreasing significantly mechanical strength.

The best mechanical properties (close to 1.6 GPa) were measured in rods with a lamellar microstructure. The planar growth front led to a homogeneous microstructure, where the maximum defect size was limited to a few microns. More-

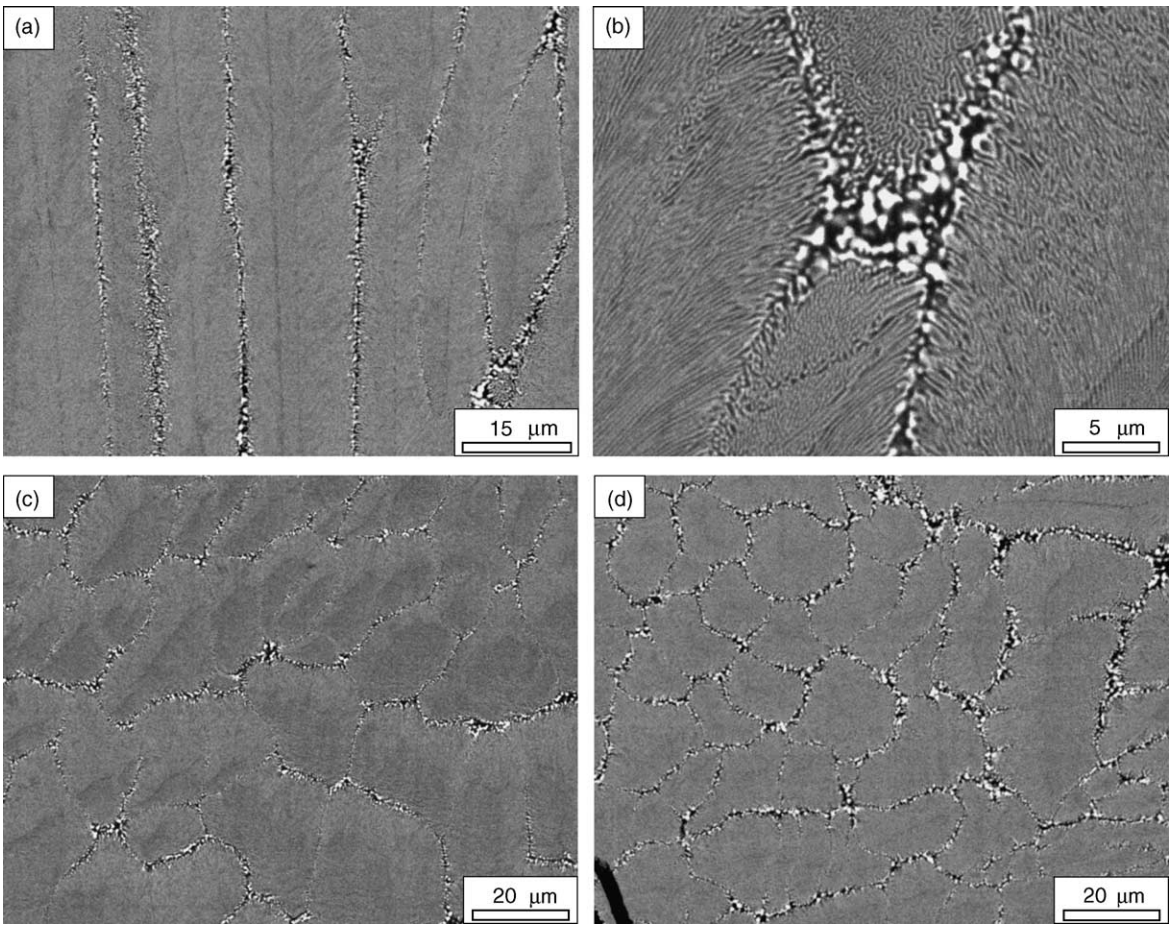

Fig. 4. Microstructure of the C3 and C12 eutectic rods grown at 1000 mm/h. (a) Longitudinal section of the C3 material, showing the cell structure elongated along the growth axis. (b) Detail of (a) showing the intercellular region and the lamellae tilting towards the cell boundary. (c) Transverse section of the C3 material showing the cell structure. (d) *Idem* for the C12 material. The micrographs were taken using back-scattered electrons to enhance the contrast between the phases.

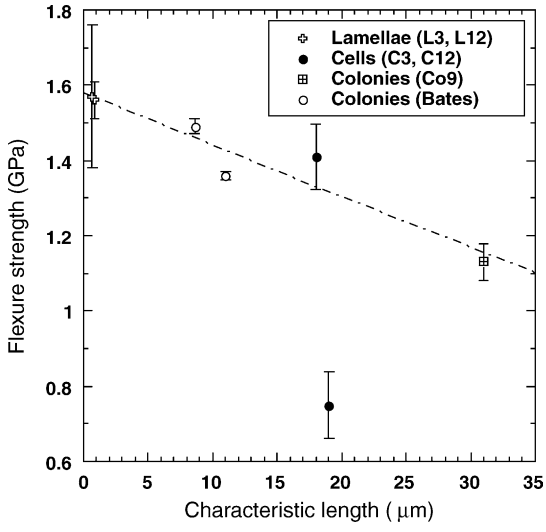

Fig. 5. Flexure strength of the eutectic rods as a function of the average characteristic length of each microstructure. See text for details.

over, no Y_2O_3 segregation occurred, and the eutectics with Y = 3% and 12% presented a similar average flexure strength in accordance with a previous investigation, which showed that Y_2O_3 contents above 3 mol% did not led to any noticeable change in the mechanical properties of Al_2O_3–ZrO_2 eutectics with a lamellar microstructure.[10] Finally, it should be noted that these average values are the highest reported in the literature for Al_2O_3–$ZrO_2(Y_2O_3)$ eutectics processed by either the laser-heated floating zone method[6–7] or the edge defined-film fed-growth method,[5] and are very likely close to the upper limit of the ambient temperature strength in bulk specimens of this system. Of course, higher strengths may be achieved in fibers of small diameter (<300 μm), due to the size effect induced by the small fiber diameter.

4.2. Weibull parameters

From the viewpoint of engineering design with brittle ceramics, the Weibull modulus of the strength is as important as the average strength. Thus, the Weibull modulus of flexure strength was determined for the L3, L12, C3, and C12 eutec-

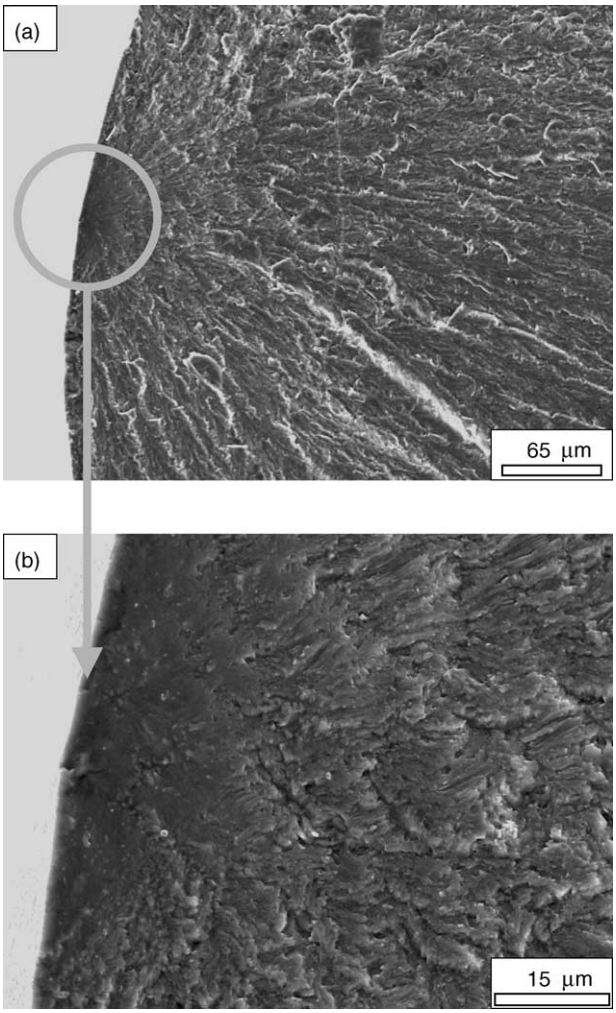

Fig. 6. Fracture surface of a C3 specimen broken at 1.48 GPa. (a) Low magnification, (b) high magnification, showing the surface defect which nucleated the fracture.

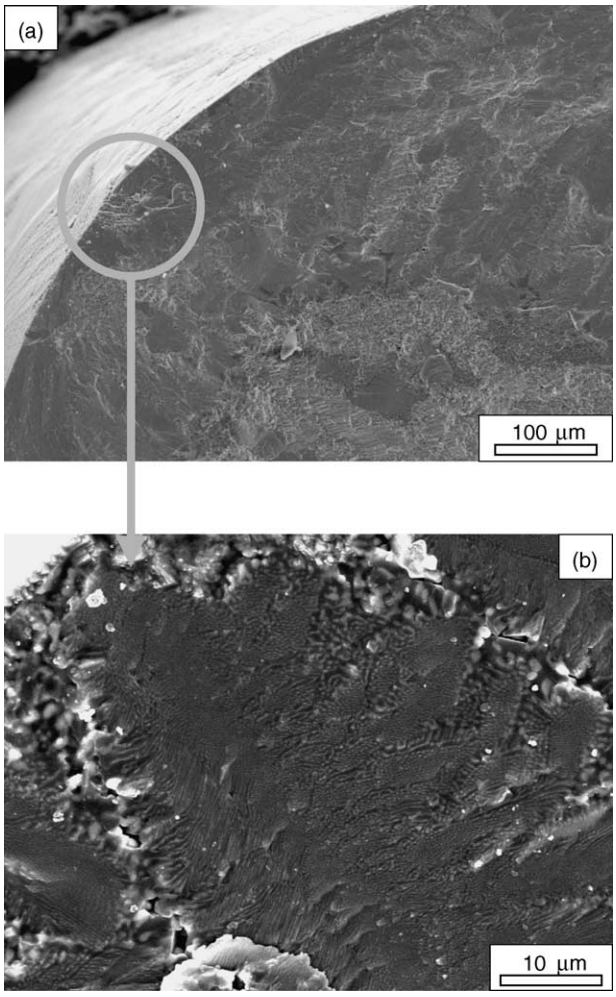

Fig. 7. Fracture surface of a C12 specimen broken at 0.52 GPa. (a) Low magnification, (b) high magnification, showing the surface defect, which nucleated the fracture.

tic rods, as shown in Fig. 8 together with the corresponding Weibull plots, where σ_f and F stand, respectively, for the flexure strength (in MPa) and the failure probability. The eutectic rods with a cellular structure (Fig. 8a) presented low Weibull moduli (between 3 and 4) which are in agreement with the distribution of cell diameters in the microstructure presented in Table 2: the standard deviation of $\pm 5\,\mu m$ indicates that cells as small as $5\,\mu m$ in diameter and as large as $30\,\mu m$ could be found, which leads to a wide population of defects and to a poor Weibull modulus. The advantage of a homogeneous, lamellar microstructure is shown in Fig. 8b, where the Weibull modulus of the L12 eutectic was close to 13, an excellent value for a brittle ceramic material, the result of the extremely fine and uniform microstructure depicted in Fig. 2c. It should be noted, however, that any loss in the homogeneity of the microstructure greatly influenced the Weibull modulus. This is the case of the L3 eutectic, whose Weibull modulus dropped to 3.4 as a result of the presence of alternating bands of fine and coarse lamellae. Although the number of flexure tests was limited, the flexure strengths measured on these samples appeared to be divided in two groups, one with high strength (>2 GPa) and the other with low strength (<1.2 GPa). The former represent the specimens which failed from the region with a homogeneous, fine lamella microstructure while the latter stand for those specimens in which fracture was nucleated by the pores and defects found at the sharp transition between bands with fine and coarse lamellae (Fig. 2b).

4.3. Hardness

The average hardness values measured on the longitudinal sections of the rods are shown in Table 3 together with the corresponding standard errors. Hardness increases as the microstructure becomes finer,[15] and the highest values were measured in the L3, L12, C3 and C12 eutectics, whose microstructure was mostly made up of a fine dispersion of ZrO_2 lamellae within the Al_2O_3 matrix. The Co9 eutectic with a colony microstructure did not reach the same hardness on account of the presence of the coarse, intercolony regions, which occupied a significant fraction ($\approx$1/3) of the sample.

Table 3
Hardness measured on longitudinal sections

	Denomination				
	L3	L12	Co9	C3	C12
Hardness (GPa)	18.3 ± 0.2	18.5±0.2	14.6±0.1	18.3±0.1	18.2±0.2

Hardness testing subjects the material mainly to compressive stresses and it is not very sensitive to the presence of cracks, so it is not surprising that that the marked differences in strength between the C3 and C12 samples (induced by the presence of pores and shrinkage cracks at the intercellular boundaries) was not detected in the hardness tests. The hardness values measured on transverse sections were practically superposed on those obtained in the longitudinal ones, and were not shown for the sake of brevity. This was as expected, as the size and spacing of the ZrO_2 lamellae in the longitudinal and transverse sections was quite similar (compare Fig. 1a and b of the L12 eutectic and 4b and 4c of the C3 eutectic).

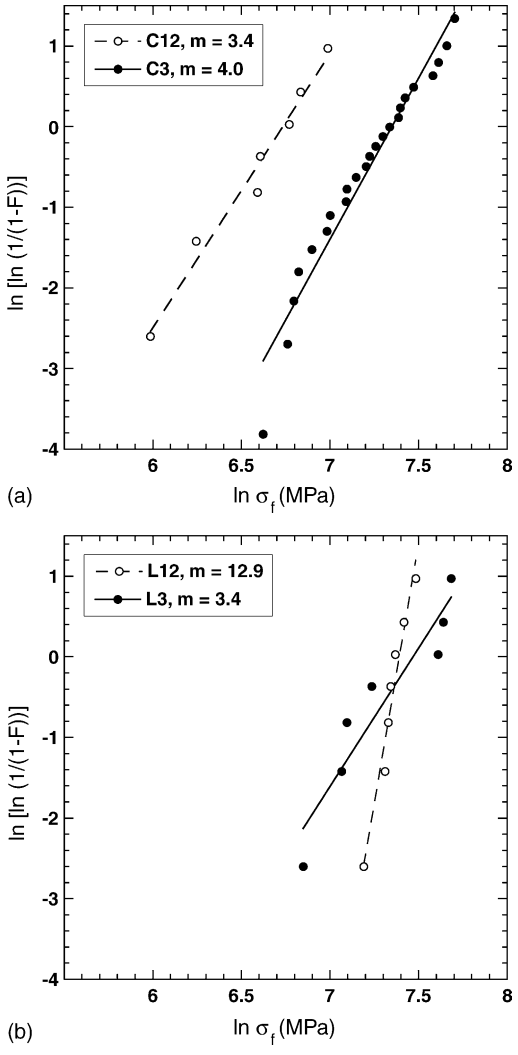

Fig. 8. Weibull plots of the flexure strength. (a) Eutectics with cellular microstructure. (b) Eutectics with homogeneous, lamellar microstructure. F stands for the failure probability and σ_f for the flexure strength in MPa.

5. Summary and Conclusions

Al_2O_3–$ZrO_2(Y_2O_3)$ eutectic rods were grown by the laser-heated floating zone method at different rates to study the effect of the microstructure on the mechanical properties. Rods grown at 20 mm/h were made up of a homogeneous dispersion of irregular ZrO_2 lamellae embedded within the Al_2O_3 matrix. This microstructure was substituted by colonies oriented perpendicularly to the solidification front at 30 mm/h. The colony core showed a dispersion of submicron ZrO_2 lamellae or rods and it was surrounded by a thick intercolony region formed by coarse ZrO_2 particles of irregular shape, where cracks and pores were sometimes found. The microstructure of the rods grown at 1000 mm/h revealed very long cells oriented along the growth axis. The cells were formed by a dispersion of very fine ZrO_2 lamellae and were separated by thin intercellular boundaries where small defects (cracks and pores) were also found.

The flexure strength of the rods was measured by three-point bending, and the best average values (close to 1.6 GPa) were obtained in the rods whose microstructure was formed by a homogeneous dispersion of ZrO_2 lamellae. The average flexure strength decreased with the increase of the size of the microstructural feature, which defined the morphology of the microstructure perpendicularly to the tensile stress. Thus, after that of rods formed by a homogeneous dispersion of ZrO_2 lamellae, the highest strength was measured in rods made up of long cells, followed by those with a colony microstructure. The rods with a cellular morphology and Y = 12%, which presented the lowest strength, were the only exception, and an explanation was found on examining the fracture surfaces. Fracture of the eutectic rods was normally nucleated at pores or cracks very close to the surface but it was triggered by the coalescence of the pores and shrinkage cavities concentrated at the intercellular region in the eutectics with cellular structure and high Y_2O_3 content.

The Weibull modulus was also determined in the eutectics with lamellar and cellular microstructure. The distribution of cell sizes in the latter was very wide (between a minimum of ≈5 μm and a maximum of ≈30 μm) and this induced a large variability in the critical defect size and reduced the Weibull modulus. On the contrary, the L3 eutectic made up of a homogeneous dispersion of ZrO_2 lamellae, whose maximum width was limited to 1.5–2 μm, presented a Weibull modu-

lus of 12.9, excellent in a brittle ceramic. It should be noted, however, that this parameter was very sensitive to the homogeneity of the microstructure, and decreased to 3.4 in the L12 rods—which had the same average strength and lamellae width—but whose microstructure was formed by alternating bands of fine and coarse lamellae.

Acknowledgements

The financial support from Spanish Ministry of Science and Technology through grants MAT2000-1533-C03-01 and 02 and from the Autonomous Government of Madrid through grant GR/MAT/0357/2004 is gratefully acknowledged.

References

1. Hulse, C. O. and Batt, J. A. *Effects of eutectic microstructures on the mechanical properties of ceramic oxides*. Report UARL N-910803-10, 1974.
2. Mazerolles, L., Michel, D. and Portier, R., Microstructure and mechanical behaviour of Al_2O_3–$ZrO_2(Y_2O_3)$ oriented eutectics. *J. Phys.*, 1986, 47.
3. Borodin, V. A., Starostin, M. Y u. and Yalovets, Y. N., Structure and related mechanical properties of shaped eutectic Al_2O_3–$ZrO_2(Y_2O_3)$ composites. *J. Cryst. Growth*, 1990, **190**, 148–153.
4. Homeny, J. and Nick, J. J., Microstructure-property relations of alumina–zirconia eutectic ceramics. *Mater. Sci. Eng. A*, 1990, **A127**, 123–133.
5. Bates, H. E., EFG growth of alumina-zirconia fiber. *Ceram. Eng. Sci. Proc.*, 1992, **13**(7/8), 190–197.
6. Courtright, E. L., Haggerty, J. S. and Sigalovsky, J., Controlling microstructures in Al_2O_3–$ZrO_2(Y_2O_3)$ eutectic fibers. *Ceram. Eng. Sci. Proc.*, 1993, **14**(7/8), 671–681.
7. Farmer, S. C., Sayir, A. and Dickerson, P. O., Mechanical and microstructural characterization of directionally-solidified alumina-zirconia eutectic fibers. *In situ Composites Science and Technology*. TMS, Warrendale, PA, USA, 1993, pp. 167–182.
8. Pastor, J. Y., Poza, P., LLorca, J., Peña, J. I., Merino, R. I. and Orera, V. M., Mechanical properties of directionally solidified Al_2O_3–$ZrO_2(Y_2O_3)$ eutectics. *Mater. Sci. Eng. A*, 2001, **A308**, 241–249.
9. Sayir, A., Farmer, S. C., Dickerson, P. O. and Yun, H. M., High temperature mechanical properties of $Al_2O_3/ZrO_2(Y_2O_3)$ fibers. *Mater. Res. Soc. Symp. Proc.*, 1995, **365**, 21–27.
10. LLorca, J., Pastor, J. Y., Poza, P., Peña, J. I., Francisco, I., Larrea, A. and Orera, V. M., Influence of the Y_2O_3 content and temperature on the mechanical properties of melt grown Al_2O_3/ZrO_2 eutectics. *J. Am. Ceram. Soc.*, 2004, **87**, 633–639.
11. Farmer, S. C. and Sayir, A., Tensile strength and microstructure of Al_2O_3–ZrO_2 hypo-eutectic fibers. *Eng. Fract. Mech.*, 2002, **69**, 1015–1024.
12. Peña, J. I., Merino, R. I., de la Fuente, G. F. and Orera, V. M., Aligned ZrO_2(c)–$CaZrO_3$ eutectics grown by the laser floating zone method: electrical and optical properties. *Adv. Mater.*, 1996, **8**, 909–912.
13. Peña, J. I., Merino, R. I., Harlan, N. R., Larrea, A., de la Fuente, G. F. and Orera, V. M., Microstructure of Y_2O_3 doped Al_2O_3–ZrO_2 eutectics grown by the laser floating zone method. *J. Eur. Ceram. Soc.*, 2002, **22**, 2595–2602.
14. Echigoya, J., Takabayashi, Y. and Suto, H., Hardness and fracture toughness of directionally solidified Al_2O_3–$ZrO_2(Y_2O_3)$ eutectics. *J. Mater. Sci. Lett.*, 1986, **5**, 153–154.
15. Lee, J. H., Yoshiwaka, A., Kaiden, H., Lebbou, K., Fukuda, T., Yoon, D. H. *et al.*, Microstructure of Y_2O_3 doped Al_2O_3–ZrO_2 eutectic fibers grown by the micro-pulling down method. *J. Crystal Growth*, 2001, **231**, 179–185.
16. Harlan, N. R., Merino, R. I., Peña, J. I., Larrea, A., Orera, V. M., González, C. *et al.*, Phase distribution and residual stresses in melt-grown Al_2O_3–$ZrO_2(Y_2O_3)$ eutectics. *J. Am. Ceram. Soc.*, 2002, **85**, 2025–2032.